Pneumatic non-contact topography characterization of finish-ground surfaces using multivariate projection methods

P. Koshy *, D. Grandy

Department of Mechanical Engineering, McMaster University, Hamilton, Canada

F. Klocke

Laboratory for Machine Tools and Production Engineering (WZL), RWTH Aachen University, Aachen, Germany

Abstract

This paper reports on the application of multivariate analysis methods for the non-contact topography assessment of finish-ground surfaces of roughness in the range of 0.1–0.8 μm *Ra*. The roughness information is extracted from the frequency spectrum of the back pressure signal acquired using a pneumatic gauge as the surface traverses past the nozzle. Principal Components Analysis is demonstrated to be effective in the unsupervised classification of lapped and ground surfaces of an identical nominal roughness of 0.1 μm *Ra*, even under conditions that the corresponding frequency spectra are contaminated with noise and affected by vibration. Projection to Latent Structures analyses are further shown to be capable of discriminating cylindrical ground surfaces based on along-the-lay measurements from a rotating component, and formulating multivariate regression models appropriate for process monitoring.

Key words: multivariate analysis, pneumatic gauging, roughness measurement, surface metrology

1 Introduction

The roughness of a surface has a critical influence on its function and performance in numerous applications relating to such phenomena as friction, lubrication, reflectivity, corrosion and fatigue. At the present time, roughness is predominantly quantified using mechanical stylus or optical instruments that are well suited for measurements in a laboratory. They do not however lend themselves to in-situ or in-process application in the typical harsh confines of a manufacturing environment. In this context, recent research efforts

* Corresponding author
Email address: koshy@mcmaster.ca (P. Koshy).

have focused on the development of alternative systems for the assessment of surface roughness [1,2].

One such system entails the application of a pneumatic gauge that is widely used in industry for the measurement of fine displacement. The application of a pneumatic sensor for assessing surface roughness was motivated by the observation that the reliability of pneumatic displacement measurement deteriorates significantly when the peak-to-valley height of the surface being gauged exceeds 3–5 μm [3]. The first work in this regard appears to be due to Nicolau [4] who utilized an air jet to relate the roughness of a surface to the back pressure measured using a water manometer. Further developments can be attributed to Hamouda [5] who conceived a twin jet co-axial gauging system with a view to expanding the measurement range, and to Tanner [6] who designed a pneumatic analogue of the Wheatstone bridge. Wang and Hsu [7] reported a linear relationship between the average voltage output of the pneumatic gauge and the corresponding *Ra* value of the surface characterized using a stylus instrument.

The reports above refer to the pneumatic sensor in contact with the workpiece, and the roughness estimated with respect to the nominal value of the back pressure signal. There are drawbacks to these techniques as measurement repeatability is influenced by the contact force developed between the sensor and the surface, as well as the contact initiating chatter when measuring fine surfaces. Furthermore, the surface being measured is stationary, with the unfortunate implication that it cannot be applied in-process. Woolley [8] demonstrated the application of fine pneumatic jets for mapping the two-dimensional spatial profile of a surface in a non-contact manner, at a relative speed of $\sim$0.8 m/min and a stand-off distance of several μm; the fidelity of the system was shown to deteriorate at higher relative traverse speeds.

Development of the pneumatic gauge for dynamic applications has been receiving attention of late [9], such as for the in-process detection of surface porosity in machined castings [10]. A recent work [11] focused on adapting this technology for non-contact roughness estimation by relating the frequency content of the back-pressure signal to the microgeometry of the surface moving lateral to the nozzle. In light of the air jet being impervious to the influence of cutting fluid and machining debris, the significant potential of the system for in-situ application in a machine tool environment was also demonstrated. The technique was further shown to be capable of rapid areal characterization of turned and milled surfaces with a roughness higher than $\sim$0.8 μm *Ra*; in the case of finer surfaces, the noise in the pneumatic signal was noted to obscure the signatures that correspond to roughness.

Following up on this limitation, the research presented in this paper refers to the pneumatic characterization of finish-ground surfaces of roughness ranging

from 0.1 to 0.8 μm *Ra*. The frequency content in the back pressure signal is processed using multivariate projection methods [12] so as to identify and isolate the features pertaining to the surface topography. This process entails several steps including feature extraction and reduction, and calibration followed by empirical model development. The applicability of the methods for classification, discrimination and regression are demonstrated, as a step towards integrating the pneumatic system into a manufacturing stream for enabling real-time, in-process assessment. This is envisaged to facilitate 100% inspection and/or adaptive process control, which would concurrently enhance both manufacturing productivity and product quality.

2 Working principle

The operation of the roughness sensor (Fig. 1) involves the supply of compressed air at constant pressure p_s through a control orifice O to the atmosphere through a nozzle, past a variable pressure chamber C so as to impinge on a work surface adjacent to it. A change in the stand-off distance x_i between the nozzle tip and the work surface due to relative normal displacement between them alters the flow of air as it leaves the nozzle. This is reflected as a highly sensitive change in the back pressure p_b measured using a sensitive dynamic piezoelectric pressure transducer P. As the nozzle translates lateral to the surface, the change in back pressure corresponds to the change in the air escape area, which is determined by the surface topography. The escape area is obtained by integrating the local distance from the nozzle tip to the surface over the circumference of the nozzle. The effects of the nozzle geometric parameters and operating variables on the sensor characteristics can be found in [11,13].

As indicated previously, for cut surfaces of a relatively coarse finish, frequency decomposition of the back pressure signal alone was sufficient to characterize the surfaces in terms of the amplitude of the dominant peak and the area under the frequency plot (see Fig. 2). For the assessment of finish-ground surfaces, the addition of an analysis module referring to multivariate projection methods (Fig. 1) was required in order to handle issues with the pneumatic noise and the effect of vibration. There have been attempts [14–17] at numerical modeling

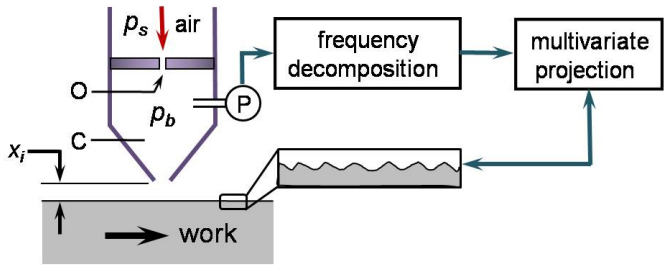

Fig. 1. *Pneumatic roughness assessment of ground surfaces.*

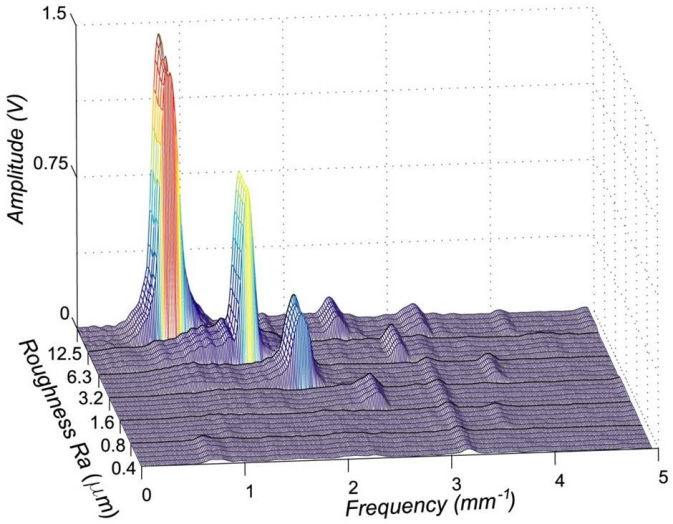

Fig. 2. *Waterfall frequency plot of pneumatic signals from milled surfaces [11].*

of the performance of pneumatic gauging systems, however these works do not consider a surface moving lateral to the nozzle. Given the lack of a fundamental physical model, it has been expedient to pursue an empirical approach in the present work.

The advantages of such a pneumatic system are several. The hardware is simple, rugged and inexpensive, and is maintenance-free on account of there being no moving parts. The sensor is also applicable to all work materials independent of such characteristics as reflectivity, and is amenable to application in confined spaces such as bore holes of a high aspect ratio that could otherwise be inaccessible. In light of it being non-contact, the technique further circumvents problems arising from contact forces and friction, thereby facilitating the assessment of moving surfaces, with potential for in-process application.

3 Experimental

The objective of the experimental work was to establish the proof of concept of pneumatic non-contact roughness assessment of moving finish-ground surfaces. To this end, the first set of experiments focussed on the capability of the system to distinguish surfaces with the same numerical roughness but different topographic attributes. For these tests, planar lapped and ground surfaces of a nominal roughness of 0.1 μm *Ra* were used, and measurements were taken at a traverse speed of 0.4 m/min. Following this, experiments were conducted in-situ on an external cylindrical grinding machine tool to collect pneumatic samples from two plunge ground surfaces of roughness 0.3 and 0.5 μm *Ra*, to test system performance when measurements are taken along the lay. The peripheral linear speed of the workpiece of diameter 58 mm was 1.5 m/min, with the nozzle traversing along the workpiece axis at a feed rate

of 12.5 mm/min such that the measurement trace was practically along the grinding lay. The last set of experiments were conducted to formulate and evaluate a multivariate regression model suitable for process monitoring. This model was created using across-the-lay measurements at a traverse speed of 0.4 m/min on flat surfaces of roughness in the range of 0.1–0.8 μm *Ra*, which were generated in a surface grinding operation.

In all experiments, the pneumatic traces corresponded to a length of at least 10 mm, and several samples were collected to capture the variability in the surface. Experiments involving flat surfaces were conducted on a die sinker with the sensor mounted on the ram of the machine tool. Back pressure measurements entailed a dynamic piezoelectric pressure transducer (Model 112A22, PCB Piezotronics) with a rise time of less than 2 μs, and a low frequency response and a resonant frequency of 0.5 Hz and 250 kHz, respectively. All experiments corresponded to nozzle and control orifice diameters of 1.5 and 0.5 mm, respectively, and a supply pressure p_s of 138 kPa. A stand-off distance $x_i = 25$ μm was chosen in consideration of the requirements referring to a non-contact application and sensor sensitivity [11,13]. The precision machine tools on which the experiments were conducted allowed the control of x_i with a resolution of 0.1 μm. The volume of the variable pressure chamber in the pneumatic sensor was $\sim$300 mm^3.

4 Assessment of ground surfaces

The difficulty with the application of the pneumatic sensor for assessing fine ground surfaces is the significant variability in the signal that is corrupted with noise. This is in contrast to the relatively repeatable and noise-free spectra (Fig. 2) corresponding to cut surfaces of a higher roughness. Fig. 3 shows the

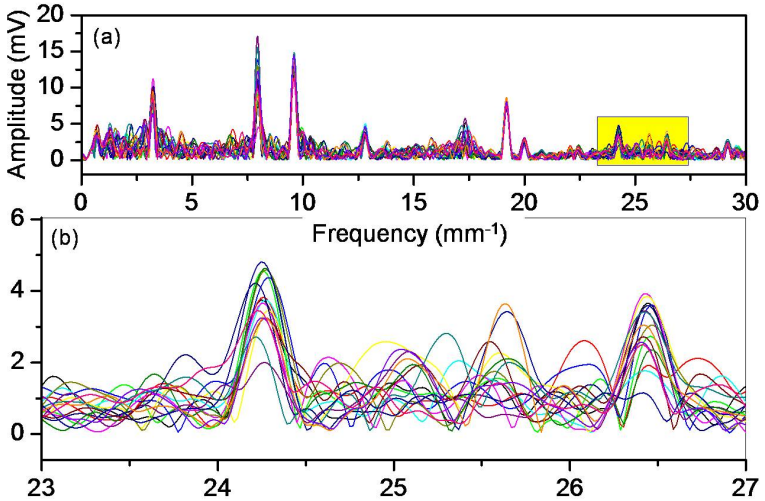

Fig. 3. *(a) Frequency plot showing 15 superimposed pneumatic signals corresponding to a flat ground surface of roughness 0.1 μm Ra; (b) shows detail of inset in (a).*

frequency spectra from 15 back pressure signals corresponding to a ground surface of roughness 0.1 μm *Ra*, with the inset showing the detail to exemplify the variability and noise. Furthermore, a comparison of a typical back pressure frequency spectrum with that of the signal from an accelerometer mounted on the moving table on which the roughness artefact was mounted, revealed a correspondence between several of the peaks in the pneumatic and acceleration signals (Fig. 4). This indicated that the pneumatic measurements are prone to be affected by vibration, particularly when measuring fine surfaces.

To address the issues above, the present work invoked two data-driven multivariate projection methods: (i) Principal Components Analysis (PCA) for the purpose of dimensionality reduction and classification, and (ii) Projection to Latent Structures (PLS) for discrimination, and the formulation of a regression model. These analysis techniques have found wide ranging applications [18,19] in chemical process industries since long; however, their application in mechanical manufacturing research has been relatively recent and few [20–22], despite their significant potential. Elements of these methods are presented in this paper with reference to their applications in the specific context of pneumatic roughness assessment of ground surfaces.

4.1 Classification of lapped and ground surfaces

Fig. 5 shows the frequency spectra from 15 back pressure signals corresponding to a lapped surface of roughness 0.1 μm *Ra*. Inspection of this data juxtaposed to that in Fig. 3 depicting data pertaining to a ground surface of the same roughness (in terms of the *Ra* parameter) makes it clear that the variability and the noise render it rather difficult to distinguish between them. PCA which is capable of dealing with large and noisy data sets with significant variability

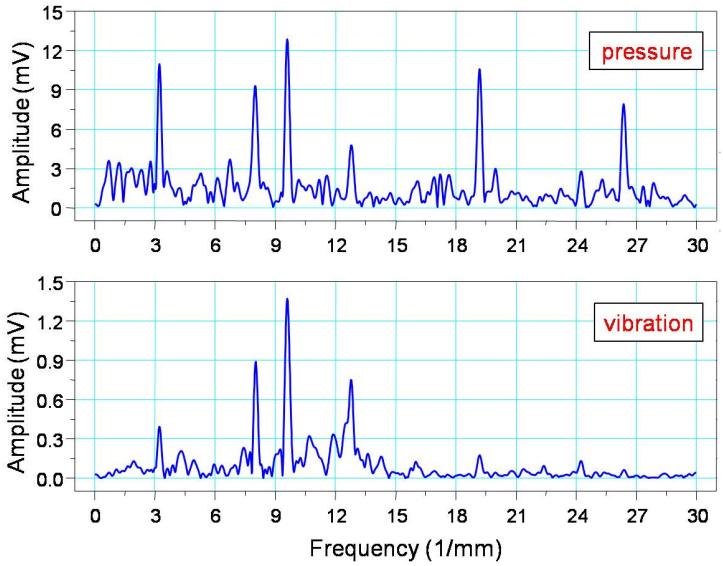

Fig. 4. *Correspondence between pressure and vibration spectra.*

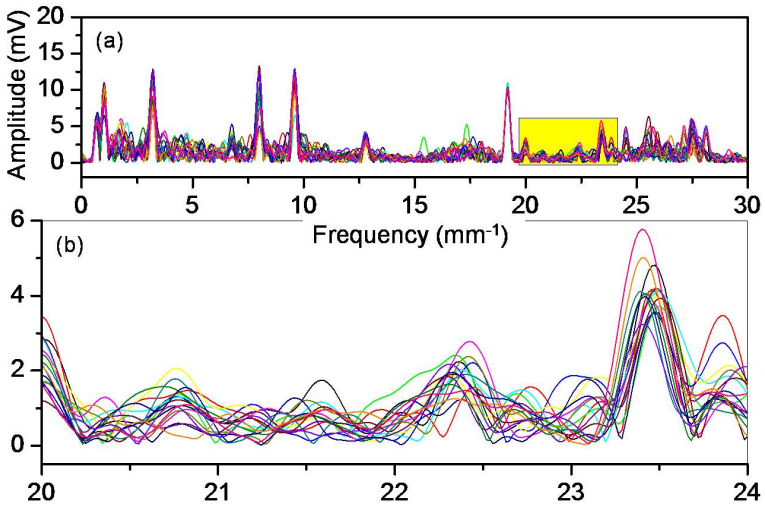

Fig. 5. *(a) Frequency plot showing 15 superimposed pneumatic signals corresponding to a flat lapped surface of roughness 0.1 μm Ra; (b) shows detail of inset in (a).*

was therefore used to analyse this data towards an attempt at unsupervised classification. This analysis technique, as will be evident shortly, is capable of identifying patterns by appropriately filtering and highlighting the pertinent information in signals contaminated with noise.

The central idea in PCA is that the dimensionality of a $(N \times K)$ data matrix $\mathbf{X}$ representing N observations and K variables can be reduced significantly by projecting it on to a lower dimensional geometric entity (such as a line or plane) to reveal clusters, trends and outliers in the data. In this work, the observations refer to several back pressure samples corresponding to ground and lapped surfaces, and the variables are the amplitudes of the back pressure signals at discrete frequencies, obtained numerically by a Fourier transformation (as seen in Figs. 3 and 5).

Geometrically, $\mathbf{X}$ represents a swarm of N data points in K-dimensional space; however, only 3 variables X_1, X_2 and X_3 are considered in the following in order to facilitate a graphical approach to explaining the essential concepts (readers are referred to [12] for a lucid presentation of the details). The N observations can be visualized in this three-dimensional space as a cloud of N points as shown in Fig. 6. The data is mean-centered, and therefore the origin of the coordinate system shown refers to the average value in the data. The data is further scaled to correspond to unit variance so as to normalize any differences in the numerical range of the variables.

The fundamental premise in PCA is that the information in $\mathbf{X}$ can be captured in a small number of independent latent variables known as principal components. The first principal component $\mathbf{t_1}$ (see Fig. 6) is a line that passes through the origin that best approximates the data swarm in the least squares

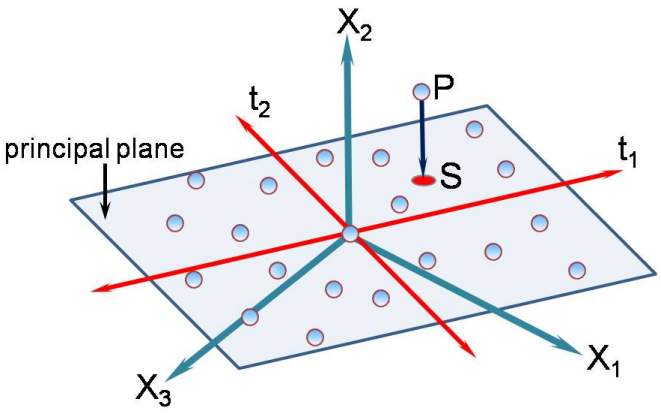

Fig. 6. *Concept of principal components.*

sense such that it corresponds to the maximum variation in the data. The second principal component $\mathbf{t_2}$ is orthogonal to the first, passes through the origin and corresponds to the next largest variation in the data, which is not captured by the first component. As variations in data are generally driven by underlying phenomena, and principal components correspond directions of maximum variance, they can be expected to reveal such phenomena that otherwise remain concealed in the data.

The two principal components define a plane in the $\mathbf{X}$-space known as the principal plane on to which each of the points in the data swarm can be projected (for example, observation P is projected to point S located on the principal plane in Fig. 6). The information in $\mathbf{X}$ is thus summarized in terms of uncorrelated principal components that are a lower-dimensional representation of the original measured variables. This concept can be extended to higher dimensions with more than just two principal components.

As the principal components are orthogonal to each other, each component offers new insight into the data. Further components could be added until the enhancement in the predictive ability of the model by the addition of another component is deemed insignificant, as evaluated by a technique known as cross-validation [12]. This entails the separation of the entire data set into several subgroups such that models can be formulated using the data devoid of one such group to predict and compare the data in the group not considered. This is repeated iteratively as many times as the number of groups to obtain an overall measure of the predictive capability of the model.

The direction of the principal components $\mathbf{t_i}$ with respect to the original co-ordinate system is specified by the loading vectors $\mathbf{p_i}$. In PCA, the $\mathbf{X}$-data is decomposed as

$$\mathbf{X} = \mathbf{T}\mathbf{P}^T + \mathbf{E} \tag{1}$$

where $\mathbf{T}$ and $\mathbf{P}$ comprise the score (coordinates of observations projected on to the principal plane) and loading vectors, and $\mathbf{E}$ refers to the residuals. $\mathbf{T}$ and $\mathbf{P}^T$ are of dimensions $(N \times A)$ and $(A \times K)$, respectively, where A is the number of principal components considered. The scores are obtained by a linear combination of the observed values in $\mathbf{X}$ and the loading vector. For instance, the first score for observation i is calculated as

$$t_{i1} = \mathbf{x}_i^T \mathbf{p}_1 \tag{2}$$

The loadings and the scores are computed recursively using the Nonlinear Iterative Partial Least Squares (NIPALS) algorithm, details of which can be found in [12].

In the present analysis, the frequency spectrum of the entire back pressure data is considered as $\mathbf{X}$. The number of observations is $N = 30$ with 15 samples each for ground and lapped surfaces. The number of variables $K = 1600$ represent the spectrum digitized in K frequencies in the range of 0 to 30 mm^{-1}, indicating that $\mathbf{X}$ is indeed a fairly large multi-dimensional data set.

The principal plane constitutes a lower-dimensional window that offers a useful perspective into the topography of the surface that is otherwise latent in the pneumatic signal. In this case, the first two principal components explained $\sim$80% of the variation in the data, and hence the 1600-dimensional roughness information in the frequency plot of the pneumatic signal could be reduced to a single point in the two-dimensional score plot (Fig. 7). Eqn. 2 implies that similar observations in the $\mathbf{X}$-space would cluster together in the score plot. This is indeed the case in Fig. 7 wherein a distinct clustering of the ground and lapped surfaces could be realized, despite the corresponding frequency spectra (Figs. 3 and 5) being contaminated with noise and affected by vibration.

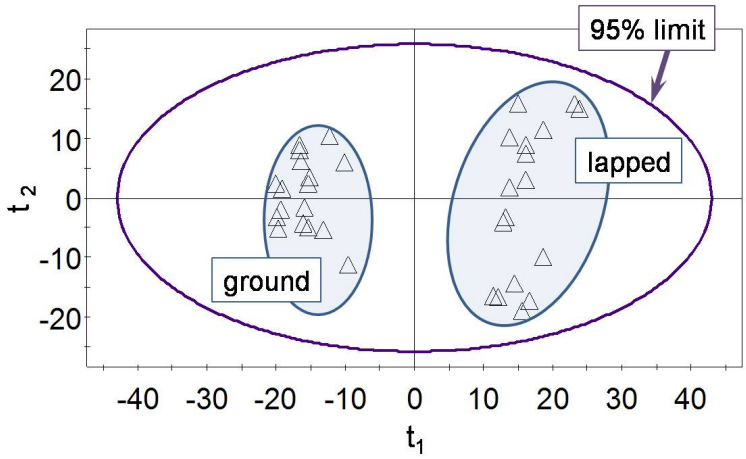

Fig. 7. *Score plot for ground and lapped surfaces of the same nominal roughness (frequency range of pneumatic signal: 0 to 30 mm^{-1}).*

The ellipse in Fig. 7 represents the 95% confidence limit for the Hotelling's T^2 statistic which is a measure of the distance of an observation from the origin in the principal plane evaluated as

$$T^2 = \frac{{t_1}^2}{{s_1}^2} + \frac{{t_2}^2}{{s_2}^2} \tag{3}$$

where ${s_i}^2$ is the estimated variance of t_i. Observations outside of the ellipse deviate from normality and would be considered outliers. In this case, all observations are bounded by the confidence limit in the model plane.

In the generation of the score plot in Fig. 7, the frequency spectra considered corresponded to a frequency range of 0 to 30 mm^{-1}, which includes both roughness and waviness components. In fact, an inspection of the lower end of the frequency spectrum in Figs. 3 and 5 point to a difference in the waviness between the ground and lapped surfaces. To filter the waviness component, PCA was repeated by omitting the contribution from the low frequency signals (less than 1.25 mm^{-1} that corresponds to a wavelength of 0.8 mm, which is the standard value [2] for a surface of roughness of 0.1 μm Ra). The corresponding score plot seen in Fig. 8 shows that the relative position of the two clusters are now different from Fig. 7, and that the ground and lapped surfaces are again well differentiated. To further test the capability of the model in classifying lapped and ground surfaces, back pressure signals that were not used in the creation of the model were input as a prediction set. The filled symbols shown in Fig. 8 refer to these data, which demonstrates that the model is indeed effective in unambiguous and unsupervised classification of new observations with reference to the frequency information in the pneumatic signal.

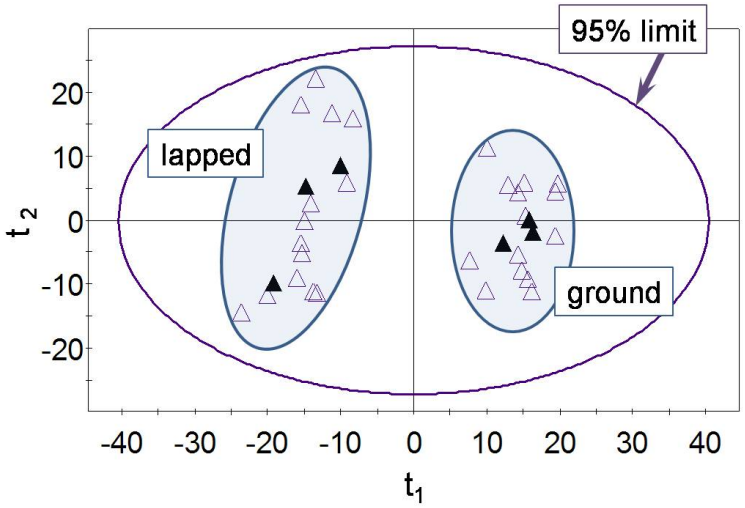

Fig. 8. *Score plot for ground and lapped surfaces of the same nominal roughness (frequency range: 1.25 to 30 mm^{-1}); filled symbols indicate test data.*

An application of the concept developed above with significant practical implication in the automotive industry refers to the problem with residual tool feed marks in finished engine cylinder bores. This is a consequence of a non-uniform and/or incomplete finish honing process that follows the boring operation. The capability of distinguishing between even lapped and finish-ground surfaces of the same numerical roughness attests to the potential of a pneumatic sensor for the in-line inspection of cylinder bores towards detecting such defects.

4.2 Discrimination of cylindrical ground surfaces

An issue with the in-process assessment of cylindrical ground surfaces is the need to halt the rotation of the component, as roughness measurements are realized across the grinding lay. It is hence of interest to investigate if cylindrical ground surfaces can be distinguished from pneumatic measurements on a rotating component, with the nozzle traversing a path almost along the grinding lay (as shown schematically in Fig. 9).

The score plot from the application of PCA on data relating to two cylindrical ground surfaces of a nominal roughness of 0.3 and 0.5 μm *Ra* (as measured across the lay with a stylus instrument) is shown in Fig. 9. Although the surfaces can be seen to have been somewhat differentiated, the separation between the clusters is not as defined as that between the ground and lapped surfaces in Figs. 7 and 8. The plot also exhibits a few outliers, which is not uncommon as the Hotelling's T^2 ellipse refers to the 95% limits. As PCA was inadequate, a technique known as Discriminant Analysis by Projection to Latent Structures (PLS-DA) was used to identify a discriminant plane that can exhibit better separation. In PLS-DA class membership information is explicitly incorporated into the model for supervised classification.

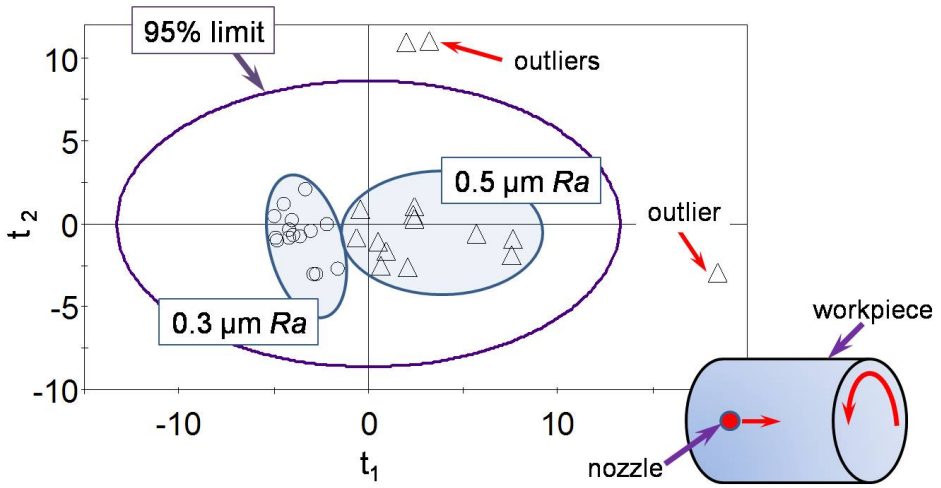

Fig. 9. *Score plot for along-the-lay pneumatic measurements on cylindrical ground surfaces of roughness 0.3 and 0.5 µm Ra.*

PLS, which can be considered a linear regression extension of PCA, is first explained in the following to lead into PLS-DA. Regression application of PLS is presented in the next section. In contrast to PCA that involves just the $\mathbf{X}$ data, PLS involves an additional matrix $\mathbf{Y}$ of dimensions $(N \times M)$ corresponding to M responses. Principal components in PCA correspond to the directions of maximum variation in the multivariate space, however these need not necessarily bring about the best separation among different classes in the data. In PLS, the first principal component $\mathbf{t_1}$ in $\mathbf{X}$-space and $\mathbf{u_1}$ in $\mathbf{Y}$-space are hence constructed (see Fig. 10) so as to: (i) explain the maximum variance in $\mathbf{X}$ and $\mathbf{Y}$, and (ii) to maximize the correlation between scores t_1 and u_1. Successive components further improve the approximations and the correlation, but with diminishing returns, and hence the increase in the spread in the data in the t_2–u_2 plot as compared to the t_1–u_1 plot (Fig. 10).

In PLS-DA, a model is developed to separate classes of observations by encoding a dummy $\mathbf{Y}$-matrix with as many columns as there are classes such that the column g is one for observations corresponding to class g, and zero for all others [12]. A PLS-DA model fit for $\mathbf{X}$ and $\mathbf{Y}$ would hence tend to separate the observations based on their respective class membership, as the information encoded in $\mathbf{Y}$ is orthogonal by design. Such an analysis can be seen to have improved the discrimination of the cylindrical ground surfaces (Fig. 11) as compared to PCA (Fig. 9).

A unique and notable feature of multivariate models is that a new observation can be checked for its consistency with the already available $\mathbf{X}$-model, before a classification is attempted. To test this feature, signals from pneumatic measurements taken across the lay (with a stationary workpiece) on a cylindrical surface of roughness 0.3 μm Ra were assessed using the PLS-DA model presented in Fig. 11 for along-the-lay measurements. The resulting score plot in

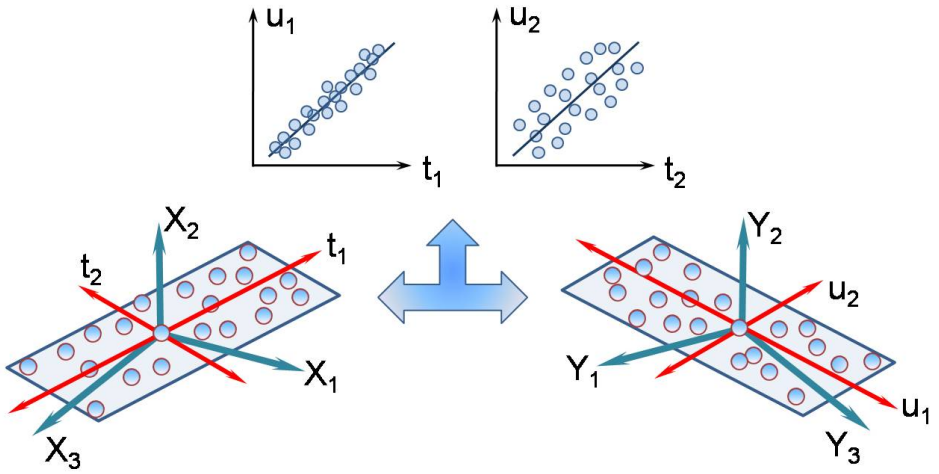

Fig. 10. *Concept of Projection to Latent Structures (PLS).*

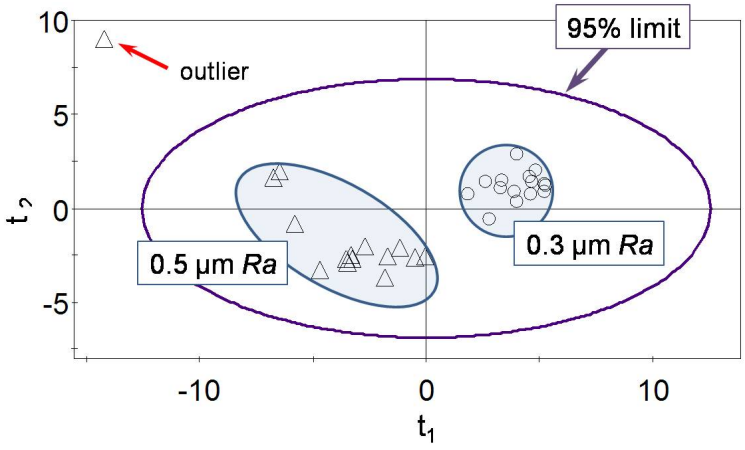

Fig. 11. *Score plot referring to partial least squares discriminant analysis (PLS-DA) of along-the-lay pneumatic measurements on cylindrical ground surfaces.*

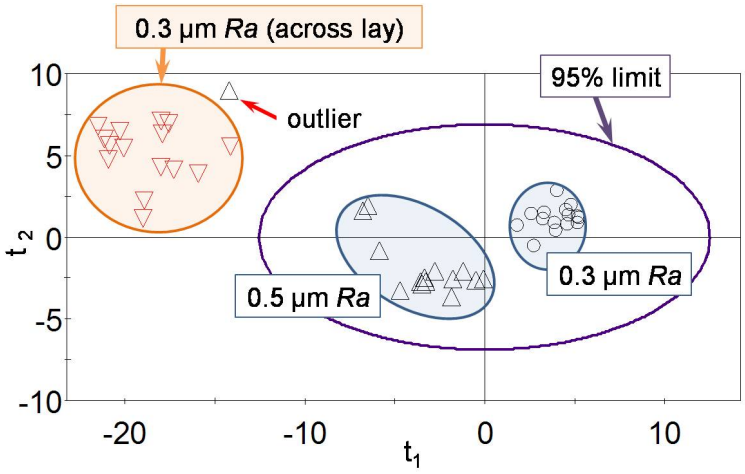

Fig. 12. *Score plot of data corresponding to across-the-lay measurements on a surface of roughness 0.3 µm Ra not included in the PLS-DA model shown in Fig. 11.*

Fig. 12 shows that across-the-lay observations cluster in the model plane, but fall well outside the 95% ellipse, signifying their lack of conformance to the model, as is to be expected.

In addition to assessing new observations before classification with respect to their projections on the principal plane as above, they can also be appraised in terms of the corresponding normalized distances to the principal plane (e.g. distance PS in Fig. 6) in the **X**-space, as shown in Fig. 13. It is amply evident that the observations corresponding to across-the-lay measurements exceed the critical distance appreciably (referring to 5% probability) in respect of the original model based on measurements taken along the lay. Such means to assess data consistency towards identifying anomalous signals enhances the robustness of multivariate methods in comparison to techniques such as neural networks. This aspect is of critical importance in process monitoring

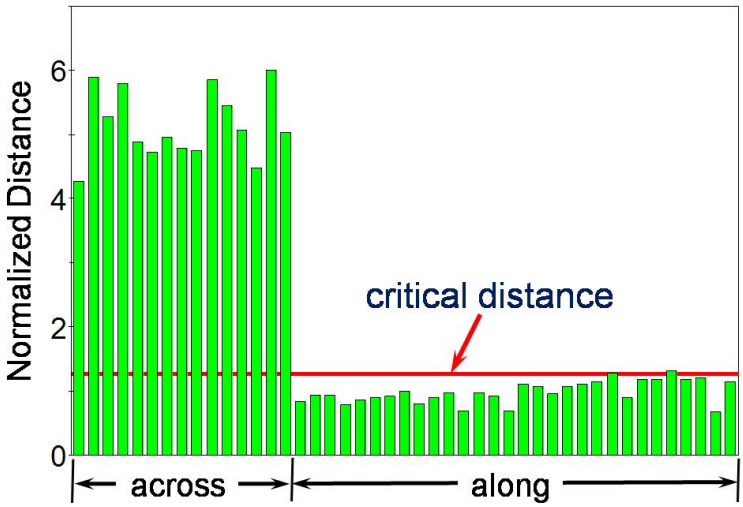

Fig. 13. *Normalized distance to model plane plot for measurements along and across the lay.*

applications.

4.3 Characterization of flat ground surfaces

This section refers to the application of PLS to relate the relevant features of the pneumatic back-pressure signal to the roughness of ground surfaces in the range of 0.1–0.8 μm *Ra*. This technique models the correlation structure in the data, and on calibration is useful for purposes of monitoring as long as this correlation structure is maintained. As shown in the previous section, the conformance of a new observation in terms of this correlation structure can be ascertained to ensure that the system performance is robust. For a single roughness parameter such as *Ra*, the $\mathbf{Y}$-matrix reduces to a vector comprising the roughness values, as opposed to the dummy matrix used for Discriminant Analysis (Sec. 4.2).

PLS regression is preferred over multiple linear regression (MLR) in light of the fact that the data is likely collinear when a large number of variables are involved, such as in this work. MLR is applicable only when $\mathbf{Y}$ is a vector and $\mathbf{X}$ is of full rank with at least $(K + 1)$ observations, which is not trivial when it comes to multivariate calibration problems. PLS is well suited for the analysis and calibration of data wherein the number of variables far exceeds the number of observations. It can further deal with collinear data as the regression is realized in terms of the latent variables that are orthogonal and hence independent of each other. The correlation between $\mathbf{X}$ and $\mathbf{Y}$ has also been explicitly considered when extracting the principal components. Although not relevant to this application, PLS is also tolerant to moderate levels (on the order of 10 to 20%) of missing data provided the data loss is not systematic [12].

On having formulated a PLS regression model, a new observation is first examined for the consistency of its structure with respect to the already conceived **X**-model in terms of the Hotelling's T^2 and Distance to Model Plane parameters described in the previous section. Following this, the relationship between **t** and **u** is used (see Fig. 10) to compute the **u** vector for this observation, which in turn can be used to make a prediction in the **Y** space.

Fig. 14 shows a comparison of the actual and predicted roughness values, which reinforces the applicability of the PLS regression model for process monitoring through appropriate multivariate calibration. The plot shows some overlap at the lower end of roughness, between surfaces of roughness 0.1 and 0.2 μm *Ra*. Model performance can be further improved by restricting the range of roughness values considered (Fig. 15).

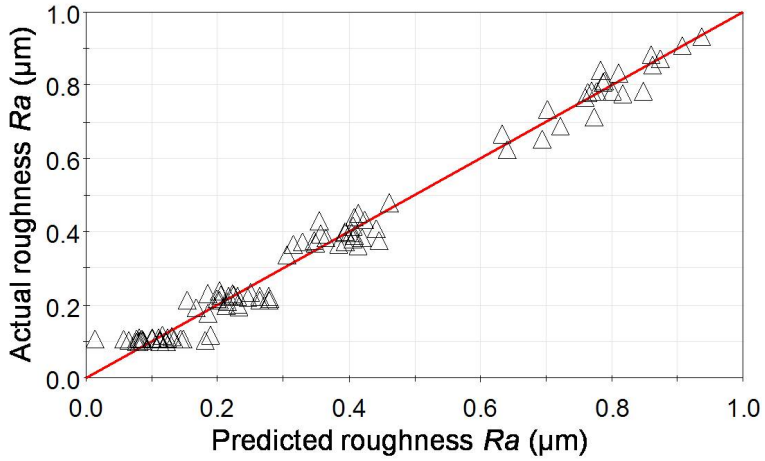

Fig. 14. *Predicted and actual roughness values of ground surfaces in the range of 0.1 to 0.8 μm Ra.*

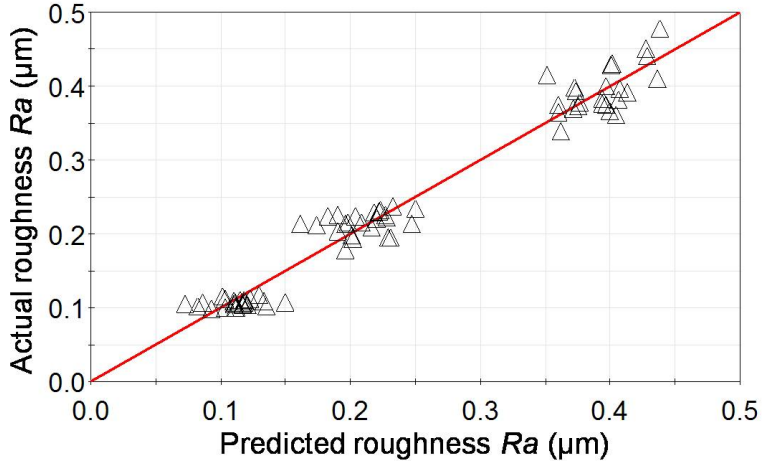

Fig. 15. *Predicted and actual roughness values of ground surfaces in the range of 0.1 to 0.4 μm Ra.*

5 Conclusions

The feasibility of applying multivariate techniques such as PCA and PLS for the non-contact pneumatic characterization of moving finish-ground surfaces has been demonstrated. Through the application of PCA, it has been possible to distinguish between ground and lapped surfaces of an identical roughness of 0.1 μm *Ra* in an unsupervised manner. PLS-DA was shown to discriminate between cylindrical ground surfaces of roughness 0.3 and 0.5 μm *Ra* based on pneumatic measurement traces taken practically along the lay, which demonstrates the potential for its in-process application in cylindrical grinding machine tools. In both cases above, model performance was evaluated and ascertained in terms of classification and prediction by using test samples that were not included in the formulation of the model. The application of a PLS regression model for ground surfaces of roughness in the range of 0.1 to 0.8 μm *Ra* has also been demonstrated.

In consideration of the enabling aspects of the technology, and the volume and range of the manufactured products with roughness specifications, the potential of the system for in-situ or in-process monitoring cannot be overemphasized. Further related work will focus on engineering the pneumatic sensor for enhanced performance, and gaining a fundamental understanding of the roughness information in the back pressure signal by means of computational fluid dynamics modeling.

Acknowledgments

This work was funded by the Natural Sciences and Engineering Research Council of Canada. P. Koshy acknowledges a fellowship from the Alexander von Humboldt Foundation. The contribution of Dr. F. Yacoub in introducing the authors to multivariate methods is appreciated.

References

[1] P.M. Lonardo, D.A. Lucca, L. De Chiffre, Emerging trends in surface metrology, CIRP Annals 51 (2002) 701–723.

[2] D. Whitehouse, 2002, Surfaces and Their Measurement, Taylor and Francis, New York.

[3] H.K. Tönshoff, I. Inasaki (eds.), 2001, Sensors in Manufacturing, Wiley-VCH, Weinheim.

[4] P. Nicolau, Applications du micrometre Solex a la mesure des etats de surface, Revue de Mecanique 21 (1937) 80–83.

[5] A.M. Hamouda, A precise pneumatic co-axial jet gauging system for surface roughness measurements, Precision Engineering 1 (1979) 95–100.

[6] L.H. Tanner, A self-balancing pneumatic Wheatstone bridge for surface roughness measurement, Wear 83 (1982) 37–47.

[7] S. Wang, K.B. Hsu, Study of pneumatic gauging to surface roughness measurement, Journal of the Chinese Society of Mechanical Engineers 8 (1987) 347–363.

[8] R. Woolley, Pneumatic method for making fast, high resolution non-contacting measurement of surface topography, Proceedings of the SPIE 1573 (1991) 205–215.

[9] M. Rucki, Step response of the air gauge, Metrology and Measurement Systems 14 (2007) 429-436.

[10] I. Menzies, P. Koshy, In-process detection of surface porosity in machined castings, International Journal of Machine Tools and Manufacture 49 (2009) 530–535.

[11] D. Grandy, P. Koshy, F. Klocke, Pneumatic non-contact roughness assessment of moving surfaces, CIRP Annals 58 (2009) 515–518.

[12] L. Eriksson, E. Johansson, N. Kettaneh-Wold, S. Wold, 1999, Introduction to Multi- and Mega-variate Data Analysis using Projection Methods, Umetrics AB, Sweden.

[13] E.O. Doebelin, 2003, Measurement Systems: Application and Design, McGraw Hill, New York.

[14] J.Y.M. Chew, S.S.S. Cardoso, W.R. Paterson, D.I. Wilson, CFD studies of dynamic gauging, Chemical Engineering Science 59 (2004) 3381-3398.

[15] C. Crnojevic, G. Roy, A. Bettahar, P. Florent, The influence of regulator diameter and injection nozzle geometry on the flow structure in pneumatic dimensional control systems, Journal of Fluids Engineering 119 (1997) 609-615.

[16] S.C.M. Yu, H.J. Poh, C.P. Tso, Numerical simulation on the flow structure around the injection nozzles for pneumatic dimensional control systems, Journal of Fluids Engineering 122 (2000) 735-742.

[17] G. Roy, D. Vo-Ngoc, D.N. Nguyen, P. Florent, Behavior of radial incompressible flow in pneumatic dimensional control systems, Journal of Fluids Engineering 125 (2003) 843-850.

[18] T. Kourti, J.F. MacGregor, Process analysis, monitoring and diagnosis, using multivariate projection methods, Chemometrics and Intelligent Laboratory Systems 28 (1995) 3-21.

[19] J.F. MacGregor, H. Yu, S.G. Munoz, J. Flores-Cerrillo, Data-based latent variable methods for process analysis, monitoring and control, Computers and Chemical Engineering 29 (2005) 1217-1223.

[20] G. Lorenz, Principal component analysis in technology, CIRP Annals 38 (1989) 107-109.

[21] A. Aggarwal, H. Singh, P. Kumar, M. Singh, Multicharacteristic optimization of CNC turned parts using principal components analysis, International Journal of Machining and Machinability of Materials 3 (2008) 208-223.

[22] S.K. Gauri, S. Chakraborty, Multi-response optimization of wire EDM using principal components analysis, International Journal of Advanced Manufacturing Technology 41 (2009) 741-748.